Journal of Sound and Vibration (2002) **255**(5), 805–817
doi:10.1006/jsvi.2001.4120, available online at http://www.idealibrary.com on IDEAL®

ON PROPER ORTHOGONAL CO-ORDINATES AS INDICATORS OF MODAL ACTIVITY

B. F. Feeny

Department of Mechanical Engineering, Michigan State University, 2555 *Engineering Building, East Lansing, MI* 48824 *U.S.A. E-mail: feeny@me.msu.edu*

(*Received* 1 *March* 2001, *and in final form* 1 *November* 2001)

Proper orthogonal decomposition (POD) is applied for examining modal activity. The extraction of proper orthogonal modal co-ordinates (POCs) is outlined. The proper orthogonal values (POVs) are the mean squared values of the POCs. The number of POVs above the noise floor provides a bound on the number of significant modes based on POVs above the noise floor. The ideas are illustrated on a linear cantilevered beam experiment. The displacement ensembles are obtained by processing six strain measurements. Coherent proper orthogonal modes (POMs) and POVs above the noise floor together confirm that six active modes are detected in the system. The distribution of modal components in POCs is discussed. The characteristics of the POMs, POVs and POCs are then examined in the presence of added noise.

1. INTRODUCTION

This paper is about the application of proper orthogonal decomposition (POD) for obtaining information about the active or significant states of a vibration system.

Proper orthogonal decomposition, also known as Karhunen–Loève decomposition and principal component analysis, is a statistical method of finding optimal distributions of energy from a set of measurement histories. POD has become a standard tool in turbulence studies since being applied by Lumley [1]. POD provides a measure of spatial coherence [1–3], and can be used to estimate the active dimension of a dynamical system [3, 4]. It is used to produce empirical modes for modal reduction of non-linear systems [5–10], and can aid in system identification [11, 12] and in some cases modal analysis [13–15].

POD is a statistical method applied to the correlation matrix derived from a set of measurement histories. POD results in a set of proper orthogonal modes (POMs) and proper orthogonal values (POVs). POMs are the optimal distributions of signal power, and POVs indicate the amount of signal power associated with the corresponding POMs. Proper orthogonal modal co-ordinates (POCs) can be defined by using POMs as basis functions. As such, the POVs turn out to be the mean squared values of the corresponding POCs, and the POVs can thus be used to gage the significance of activity associated with the corresponding POMs.

Using the POVs, the POMs can be ranked in descending order of signal power. The cumulative power then is the truncated sum of the POVs. It has been customary to say that the number of significant, or active, modes are those of the largest power that contain, say, 99% or 99·9% of the total signal power [1, 3, 4, 8, 16]. This is a prescribed criterion. The chosen number varies with the problem at hand and the insight of the researcher.

0022-460X/02/000000 + 13 $35.00/0

In this paper, we explore the usage of POCs to assess modal activity. Specifically, we examine the meaning, in terms of the number of active modes, of POVs above the noise floor. We look at the POCs to see how frequency information can be obtained, and how that information helps in determining the number of active modes. These ideas are addressed in application to an experimental linear beam. We then look at the effect of added noise.

Next, we review the application of POD toward the extraction of modal activity.

2. POD AND MODAL ACTIVITY

In this section, we describe more details about the POD process, as will be applied in this work. We will borrow a criterion for the significance of modal activity from a similar tool, singular system analysis, which will therefore also be summarized.

2.1. PROPER ORTHOGONAL DECOMPOSITION

Application of POD to structures typically requires sensed dynamical quantities at M locations within the system. For this discussion, these quantities are taken to be displacements $x_1(t), x_2(t), \ldots, x_M(t)$, although other states can be used [17, 18]. When the displacements are sampled N times, we can form displacement-history arrays, such that $\boldsymbol{x}_i = (x_i(t_1), x_i(t_2), \ldots, x_i(t_N))^{\mathrm{T}}$, for $i = 1,2, \ldots, M$. (The means are sometimes subtracted from the displacement histories.) In performing the proper orthogonal decomposition, these displacement histories are used to form an $N \times M$ ensemble matrix,

$$\mathbf{X} = [\mathbf{x}_1, \mathbf{x}_2, \ldots, \mathbf{x}_M].$$

Each row of $\mathbf{X}$ represents a point in the measurement space at a particular instant in time. The $M \times M$ correlation matrix $\mathbf{R} = (1/N)\mathbf{X}^{\mathrm{T}}\mathbf{X}$ is then formed. Since $\mathbf{R}$ is real and symmetric, its eigenvectors are orthogonal. The eigenvectors $\mathbf{v}$ of $\mathbf{R}$ are the proper orthogonal modes, and the eigenvalues λ are the proper orthogonal values.

The POMs are the principal axes of inertia of the data in the measurement space, and the POVs indicate the mean squared values of the data in the directions of the corresponding POMs [13]. Equivalently, POVs indicate the signal power associated with the corresponding POMs [1, 4].

The dynamics can be decomposed into modal co-ordinates by using the POMs as basis functions [19]. To this end, we define a proper orthogonal modal matrix $\mathbf{V} = [\mathbf{v}_1 \cdots \mathbf{v}_M]$. We can define modal co-ordinates $\mathbf{q}(t)$ with elements $q_i(t)$, $i = 1, \ldots, M$, such that $\mathbf{x}(t) = \sum_{i=1}^{M} q_i(t)\mathbf{v}_i = \mathbf{V}\mathbf{q}$. As such, the ensemble matrix is $\mathbf{X} = \mathbf{Q}\mathbf{V}^{\mathrm{T}}$, where $\mathbf{Q}$ is an ensemble of proper modal co-ordinates (POCs). Thus,

$$\mathbf{Q} = [\mathbf{q}_1, \mathbf{q}_2, \ldots, \mathbf{q}_M],$$

where $\mathbf{q}_i = (q_i(t_1), q_i(t_2), \ldots, q_i(t_N))^{\mathrm{T}}$, for $i = 1, \ldots, M$, are individual modal co-ordinate histories. If $\mathbf{V}$ is normalized, then $\mathbf{V}^T\mathbf{V} = \mathbf{I}$ because of orthonormality. Thus, we can extract the POC histories $q_i(t)$ from the original ensemble $\mathbf{X}$ via $\mathbf{Q} = \mathbf{X}\mathbf{V}$. Each modal co-ordinate represents the dynamics in the axis of a corresponding POM. The mean squared value of this modal co-ordinate is the associated POV.

In the special case of linear, lightly damped systems with uniform mass distributions (or made so by a co-ordinate transformation), under a multi-modal free response, the POMs

converge to the linear normal modes (LNMs) [13, 15], approximately in the case of continuous systems [14].

If the POMs are indeed identical to the LNMs, then the POCs $q_i(t)$ and the true linear normal modal co-ordinates $\eta_i(t)$ are identical. Suppose the POMs differ from the LNMs, ϕ_i, such that $\mathbf{v}_i = \phi_i + \varepsilon_i$. Then, $\mathbf{x}(t) = \mathbf{V}\mathbf{q}(t) = [\phi_1 + \varepsilon_1, \phi_2 + \varepsilon_2, \ldots, \phi_M + \varepsilon_M]\mathbf{q}$. By orthogonality of the POMs, $\mathbf{q}(t) = \mathbf{V}^{\mathrm{T}}\mathbf{x}(t)$, whence

$$q_i(t) = \phi_i^{\mathrm{T}}\mathbf{x}(t) + \varepsilon_i^{\mathrm{T}}\mathbf{x}(t) = \eta_i(t) + \varepsilon_i^{\mathrm{T}}\mathbf{x}(t), \tag{1}$$

that is if the mass distribution is uniform such that $\phi_i^{\mathrm{T}}\phi_j = \delta_{ij}$. The error vector ε_i can be written in terms of linear normal modes by using the expansion theorem [20]: $\varepsilon_i = \sum_{j=1, j\neq i}^{M} d_j\phi_j$. Hence,

$$q_i(t) = \eta_i(t) + \sum_{j=1, j\neq i}^{M} d_j\eta_j(t). \tag{2}$$

Thus, the proper orthogonal modal co-ordinate $q_i(t)$ is polluted by other normal modal co-ordinates depending on the deviation of the POM $\mathbf{v}_i$ from the LNM ϕ_i as well as the relative strengths of linear normal modal components $\eta_j(t)$. Small deviations d_j lead to small impurities in $q_i(t)$, while large modal co-ordinate dynamics η_j increase the impurity of $q_i(t)$.

POC histories and spectra have been examined in a simulated homogeneous beam [19] and the dominant harmonic represented the modal characteristics in the lower modes of the beam. If the POMs do not represent the LNMs (e.g., if the mass distribution is not uniform [13, 14]), we cannot make a clear connection between $q_i(t)$ and $\eta_i(t)$. Furthermore, for steady state responses to harmonic excitations, the connection is absent, unless the excitation is measured and incorporated into the POD [15].

2.2. MODAL SIGNIFICANCE

We will be looking at the POVs, which are the mean squared values of POCs, and also the POCs themselves, to extract information about modal activity. We will explore a POV-based criterion for dynamical significance based on determining the number of POVs that are above the noise floor. The idea here is that POVs above the noise floor represent mean squared proper orthogonal modal dynamics that have a meaningful deterministic contribution. This criterion draws off an idea formerly applied to a similar data processing tool, singular system analysis (SSA), which was proposed for putting bounds on the number of active state variables from a single observable [21]. Subsequent studies had shown that conclusions drawn about state activities by using SSA can be erroneous.

The application of singular system analysis as presented by Broomhead and King [21] occurs not on an ensemble of distinct measurements, but rather on an ensemble of delays of a single sampled observable, $y(t_j)$, where t_j are time samples. A phase-space delay reconstruction [22, 23] is performed by forming vectors $\mathbf{s}_j = (y(t_j), y(t_{j+k}), \ldots, y(t_{j+(E-1)k}))^{\mathrm{T}}$, for $j = 1,2,\ldots,N$, in the E-dimensional delay space, where the delay k and the dimension E are chosen according to the standard methods [24]. The ensemble matrix is then $\mathbf{S} = [\mathbf{s}_1, \mathbf{s}_2, \ldots, \mathbf{s}_N]^{\mathrm{T}}$. From this, the autocorrelation matrix is then $\mathbf{R} = (1/N)\mathbf{S}^{\mathrm{T}}\mathbf{S}$. $\mathbf{R}$ has eigenvectors and eigenvalues, which are the singular vectors and squared singular values of $\mathbf{S}$. Again, the eigenvectors are the principal axes of inertia of the data in the delay space, and the eigenvalues are the mean squared values of the delay vectors in the directions of the eigenvectors.

The idea proposed originally [21] was to estimate E, and hence the number of delay co-ordinates needed to describe the data, by first choosing a reconstruction dimension larger than E, and finding the singular values above the noise level. The argument was that the ellipsoid of inertia has only as many significant axes as there are meaningful independent co-ordinates, which, in the case of phase-space delay reconstructions, are delays of a single observable. The number of significant axes would provide an estimate of E based on statistics, rather than geometry (i.e., not based on whether trajectories cross). As it turns out, in the scenario of the delay reconstruction, in which the columns of **S** come from delays of the same sampled continuous waveform, an **S** matrix of arbitrary size can have full rank, and so this criterion does not lead to an estimate of the number of independent delay co-ordinates needed to describe the data [25–28].

In the POD, the columns of **X** come from distinct, and potentially independent, measurements. If the response of a linear system with synchronous modes occurs in few modes, and a greater number of measurements are taken to build the ensemble matrix **X**, we would expect **X** to have a low rank. For example, suppose a beam vibrates in one mode, but is measured at several locations. The rank of **X** would be one.

More generally, this low rank of **X** may not hold. A synchronous non-linear normal mode, for example, would form a curve in the measurement space, and could lead to a full-rank **X**. As an example, the POD of a single synchronous normal modal response was examined for a non-linear beam simulated with five active linear modal co-ordinates [14]. The largest five POVs, 46·96, 0·1227, 0·2958e-3, 18·59e-6, and 11·34e-6, were above the noise floor. Clearly, the number of POVs above the noise floor exceeded the number of active non-linear normal modes, which was one.

3. EXPERIMENTS WITH A LINEAR BEAM

3.1. APPARATUS AND DISPLACEMENT MEASUREMENT

These experiments with a linear beam were originally conducted to test the applicability of POD as a linear modal analysis tool [29]. A cantilevered steel beam of 0·394 m length, 0·012 m width, and 0·00079 m thickness was fixed at one end in a steel clamp. The natural frequencies were found to be 4·5, 27·2, 75·5, 147, 243, and 365 Hz. The theoretical modal frequencies of the Euler-beam model were 4·5, 28·4, 79·4, 156, 257, and 384 Hz.

Six strain-gage pairs were placed along the beam to sense bending strains. The locations of the strain-gage pairs were $x_1 = 5{\cdot}27 \times 10^{-3}$ m, $x_2 = 0{\cdot}0543$ m, $x_3 = 0{\cdot}1033$ m, $x_4 = 0{\cdot}1523$ m, $x_5 = 0{\cdot}2013$ m, and $x_6 = 0{\cdot}2503$ m, measured from the clamped end. The strain gages were biased toward the clamp for strain sensitivity, while the desired displacement locations are to be equally spaced from clamp to tip, to satisfy a condition for the approximation of LNMs by POMs [14].

The strains were converted into displacement estimates in the following way. The bending strain in a symmetric beam at a location x_i is related to the transverse deflection $y(x, t)$ by

$$\varepsilon(x_i, t) = c\left[\frac{\partial^2 y(x, t)}{\partial x^2}\right]_{x = x_i}, \tag{3}$$

where c is half of the thickness of the beam. If we approximate

$$y(x, t) \approx \sum_{j=1}^{M} \phi_j(x) u_j(t), \tag{4}$$

where $\phi_j(x)$ are the basis functions that satisfy the geometric boundary conditions, and $u_j(t)$ are the generalized co-ordinates. Evaluating $y(x,t)$ at $\hat{M}$ distinct locations x_k, we can write

$$\mathbf{y} = \mathbf{\Phi u}, \tag{5}$$

where $y_k = y(x_k, t)$ are the elements of the $\hat{M}$-vector $\mathbf{y}$, $\phi_{kj} = \phi_j(x_k)$ are the elements of $\hat{M} \times M$ matrix $\mathbf{\Phi}$, x_k are the desired displacement locations, and $u_j(t)$ are the elements of M-vector $\mathbf{u}$.

Using equations (3) and (4), and evaluating at M strain-gage locations x_i, the vector of measured strains are related to modal co-ordinates by

$$\hat{\varepsilon} = c\mathbf{\Psi u}, \tag{6}$$

where the measured strains $\varepsilon_i = \varepsilon(x_i)$ are the elements of $\hat{\varepsilon}$, and $\psi_{ij} = \mathrm{d}^2\phi_j(x)/\mathrm{d}x^2|_{x=x_i}$ are the elements of $M \times M$ matrix $\mathbf{\Psi}$. As such, the generalized co-ordinates $\mathbf{u}$ can be expressed as

$$\mathbf{u} = \frac{1}{c}\mathbf{\Psi}^{-1}\hat{\varepsilon}. \tag{7}$$

Matrix $\mathbf{\Psi}$ is invertible as long as the second derivatives of the linearly independent basis functions remain independent.

Our goal is to take M strains at measured locations on the beam, and estimate $\hat{M}$ displacements at some other locations $x_1, \ldots, x_{\hat{M}}$. Thus, the $M \times M$ matrix $\mathbf{\Psi}$ is constructed based on the M actual strain-gage positions and M basis functions, and the $\hat{M} \times M$ matrix $\mathbf{\Phi}$ is built based on the M basis functions evaluated at $\hat{M}$ desired displacement locations. The basis functions chosen were the theoretical normal modes of a cantilevered Euler beam. (While it may seem unnecessary to perform POD when the theoretical modes are known, our purpose is not to identify modes but to illustrate the role of POCs.) The resulting vector of displacements is

$$\mathbf{y} = \frac{1}{c}\mathbf{\Phi\Psi}^{-1}\hat{\varepsilon}. \tag{8}$$

In this study, $M = 6$ and $\hat{M} = 20$. Therefore, we have 20 displacement histories (approximated via modal truncation) which are linearly dependent. There are at most six independent displacements, which can produce only six meaningful modes. The motivation for using $\hat{M} > M$ is to "improve" the spatial resolution for modal analysis [29], knowing of course that the resolution is not truly improved, rather the displacements are interpolated across the beam, using the functions $\phi_j(x)$ as a basis for the interpolation.

3.2. POMS AND POVS OF THE BEAM

The beam was excited with a simple impulse, and the ensuing free vibration was monitored. The six strain histories were simultaneously sampled and, due to nuances in the data acquisition system, recorded in 0·2 s windows which were then concatenated. These strain histories were later post-processed according to the above development to produce 20 redundant displacement histories. A total of 800 samples were recorded. As such, the ensemble matrix $\mathbf{X}$ was 800×20. The correlation matrix $\mathbf{R}$ was formed, and the POMs and POVs were extracted.

The POVs are plotted in a logarithmic scale in Figure 1. We know a priori that there are a maximum of six detectable independent modes. Everything beyond six is spurious. This is

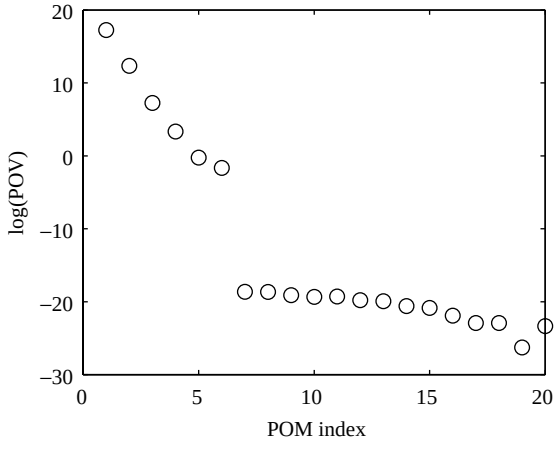

Figure 1. The logarithms of the POVs.

brought out in the logarithmic plots. The first six POVs are distinct from the spurious set. The spurious POVs are not clearly distinguishable and can be considered as noise. This suggests that there could be six meaningful modes detected in the system response.

If λ_i denotes the POVs, and Λ is their sum, then in this example $\lambda_1/\Lambda = 0{\cdot}9928$, $(\lambda_1 + \lambda_2)/\Lambda = 0{\cdot}999954$, and $(\lambda_1 + \lambda_2 + \lambda_3)/\Lambda = 0{\cdot}9999991$.

Figure 2 shows the first eight POMs plotted with circles. The first six are representative, at least qualitatively, of the first six linear normal modes of a cantilevered Euler beam, which are plotted with solid lines. The deviation could arise in the spatial resolution of the sensors, the choice of basis functions, or in the deviation of the beam from an ideal cantilevered beam. The clamp is likely to be non-ideal. The next two modes (and indeed the next 12 modes) are not coherent. The structure of the modes, while preserving the clamped boundary condition, is noisy, as the modes are generated from the noise level of the system. None of the theoretical normal modes clearly resemble the seventh and eighth POMs. The conclusion drawn from the POMs is that there are six modes captured in the system response, the maximum we expected. Thus, the POMs and POVs point to the same conclusion.

This example is special because of the clear delineation between deterministic and random modal information, and is therefore illustrative. It is not a contrived example, as the experiment was developed purposefully for modal analysis, and it involves the real situation of having a limited number of sensors.

More typically, there might be enough independent sensors for the POVs to descend into the noise level. To examine this scenario, we added random noise post partum to the displacement data. A random number was added to each displacement datum. The random signal had a uniform distribution of zero mean and a root mean squared value of 0·26% of the square root of the maximum POV. (The maximum POV indicates the mean squared value of the associated POC.)

The POD was then performed. Under such conditions, the logarithms of the POVs had the form of those plotted in Figure 3. There were clearly three POVs above the noise floor. The POVs are such that $\lambda_1/\Lambda = 0{\cdot}9927$,$(\lambda_1 + \lambda_2)/\Lambda = 0{\cdot}99983$, and $(\lambda_1 + \lambda_2 + \lambda_3)/\Lambda = 0{\cdot}99989$. The first six associated POMs are shown in Figure 4. The first three POMs were well representative of the first three linear normal modes. The subsequent POMs have no correlation with linear normal modes, and do not represent deterministic dynamical

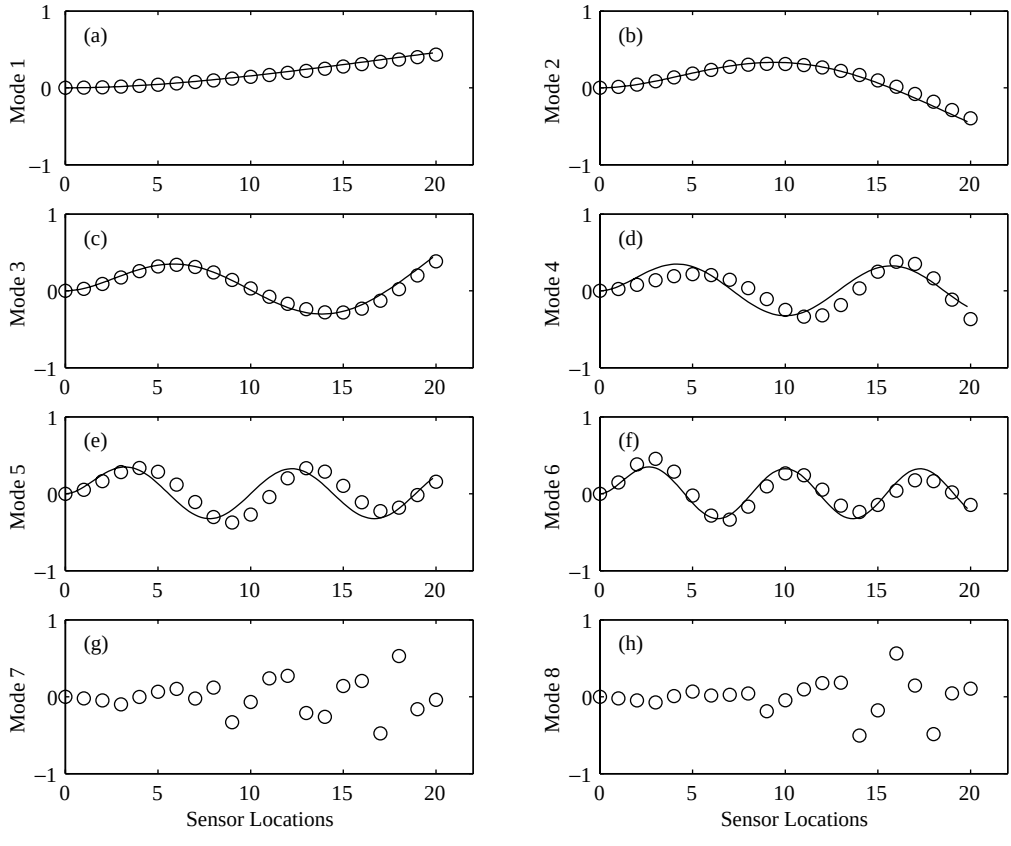

Figure 2. The first eight POMs ordered in (a)–(h) by descending POVs. The circles indicate the POMs, and the solid lines show the theoretical normal modes.

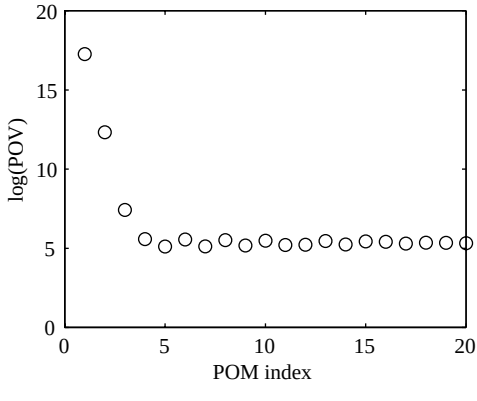

Figure 3. The logarithms of the POVs. Random noise has been added to the displacement signals.

properties. As such, three modes are identifiable, consistent with three POVs above the noise floor. The ratio of the POV noise floor to the maximum POV was 0·0028, close to the relative level of the introduced noise.

If we consider the per cent power criterion, what result would we have? In each case, undoctored and random noise added, according to the 99% criterion, we have one

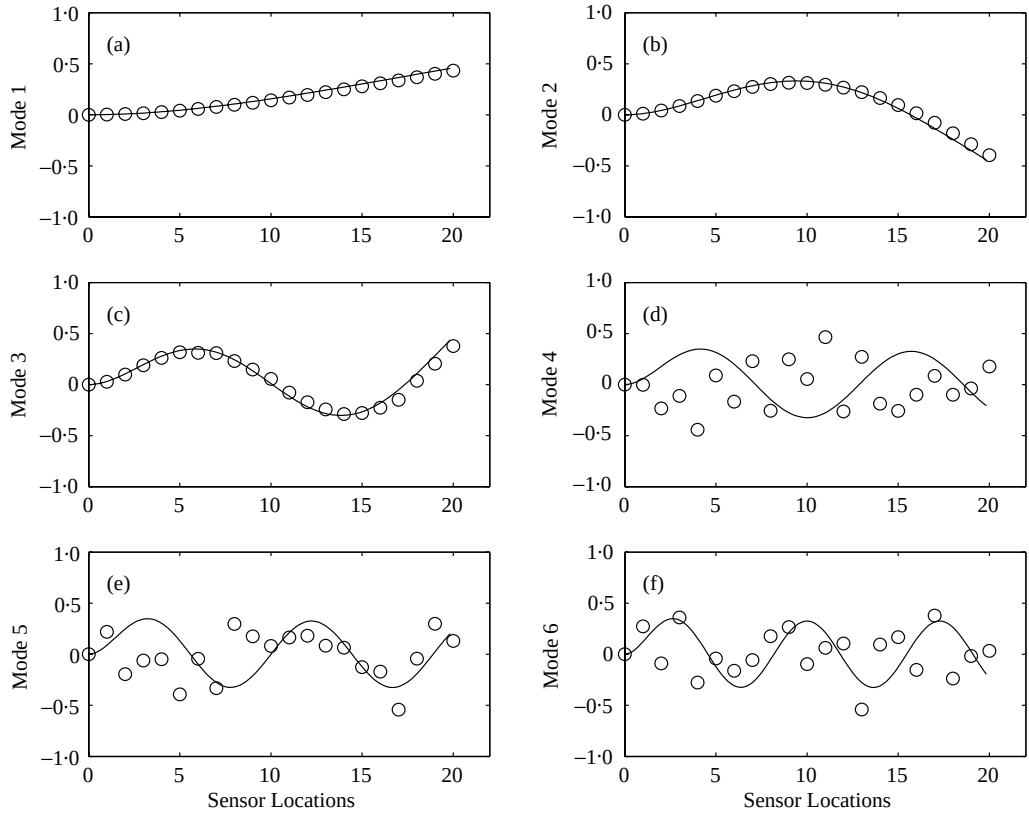

Figure 4. The first six POMs ordered in (a)–(f) by descending POVs for the case with added random noise. The circles indicate the POMs, and the solid lines show the theoretical normal modes.

significant mode. According to the 99·9 and 99·99% criteria, we have two and three significant modes (barely four modes in the noisy data). The result is different from the noise level criterion. But the per cent power criterion is a prescription, and it holds meaning toward the determination of the number of significant dominant modes. Indeed, this system, if modelled for its large-scale behavior, might aptly be described by 1–3 modes, depending on what is needed out of the model.

3.3. PROPER ORTHOGONAL CO-ORDINATES

Since our data contains 0·2 s windows of continuous sampling, we look at proper orthogonal modal co-ordinates $\mathbf{q}_i(t)$ from $\mathbf{Q} = \mathbf{XV}$ during a single continuous window, in this case the second 0·2 s of the response.

For the noise-free case the POCs are plotted in Figure 5. The visual impression is that the first six modal co-ordinate histories are distinct, and that the last two, which are spurious, give no new information in their dynamics. The first two modes seem to be dominated by harmonic components of distinct frequencies.

The fast Fourier transforms of these signals are shown in Figure 6. The first two modes are clearly dominated by the first two modal frequencies of the beam. The third mode already has a stronger component from the second linear normal mode than from the third

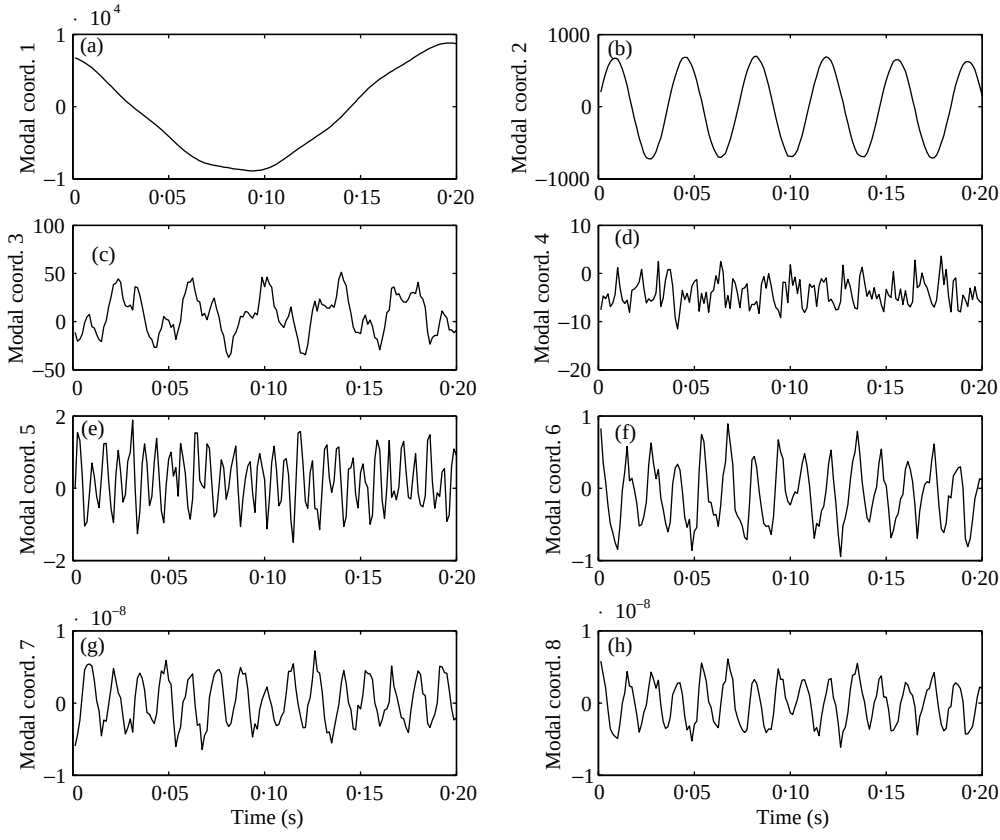

Figure 5. The proper modal co-ordinate histories for the first eight proper orthogonal modes ordered in (a)–(h) by descending POVs.

linear normal mode, judging by the frequency content. This happens because the third POM is not identical with the third LNM. Looking at the close comparison with theoretical modes in Figure 2, it may be a surprise that the third POC is dominated by the second modal frequency. It means that the contribution of the second normal mode in the third POC, that is $d_2^{(3)}\eta_2(t)$, where $d_2^{(3)}$ represents the component of the second linear normal in the third POM, is stronger than the third normal modal co-ordinate $\eta_3(t)$. However, the modal power distribution, i.e. the set of POVs, suggests that the third frequency pales in comparison to lower modal frequencies. At a glance, the fourth POC does not seem to introduce meaningful information about modal frequencies, while the fifth does, and the sixth again does not. (But this could be a matter of the vertical-axis scale.) It is likely that the six modal frequencies are present, since the six modes were well represented, but that the fifth and sixth frequency components are very small compared to the others. (If we had a longer continuous time record available, we might get more insight from the improved frequency resolution.) In this system, the POMs deviate slightly from the LNMs, and the normal modal components shuffle into the POCs according to equation (2).

The proper orthogonal modal co-ordinate histories were also examined in the noise-contaminated case. Figure 7 portrays the first four modal histories, which can be compared to the first four modal histories in the noise-free case, in Figure 5. The first two POCs have a clear representation of the respective modal dynamics. The third modal

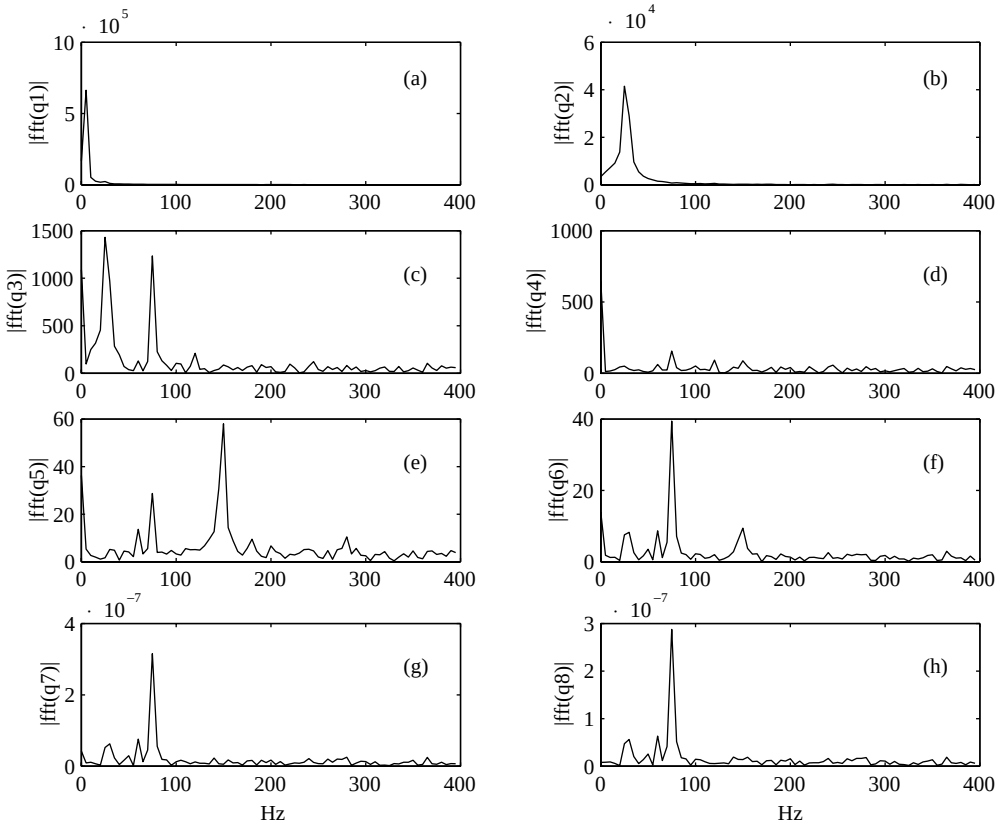

Figure 6. The Fourier transforms of the proper modal co-ordinate histories $q_i(t)$ for the first eight proper orthogonal modes ordered in (a)–(h) by descending POVs.

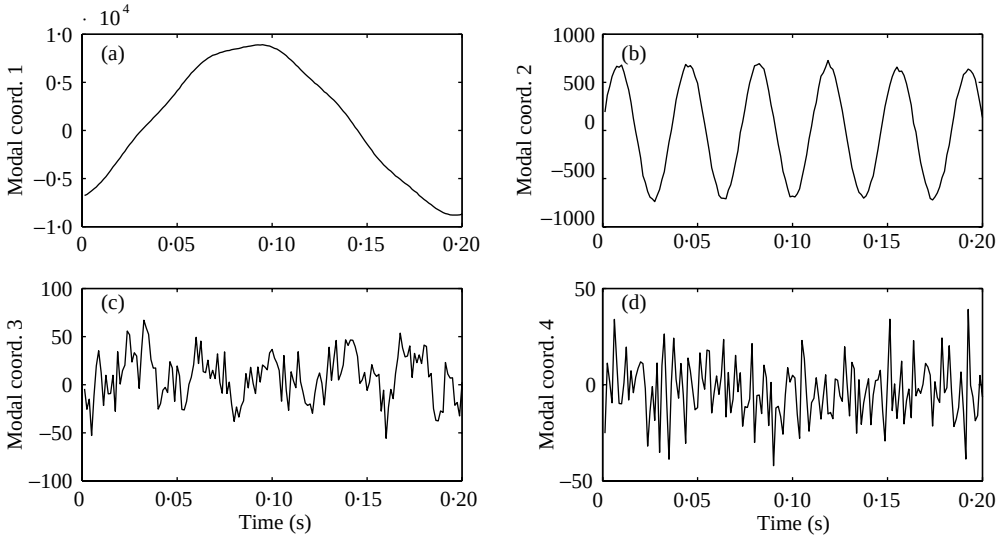

Figure 7. The proper modal co-ordinate histories for the first four proper orthogonal modes ordered in (a)–(d). In this case, there is noise added to the displacement data.

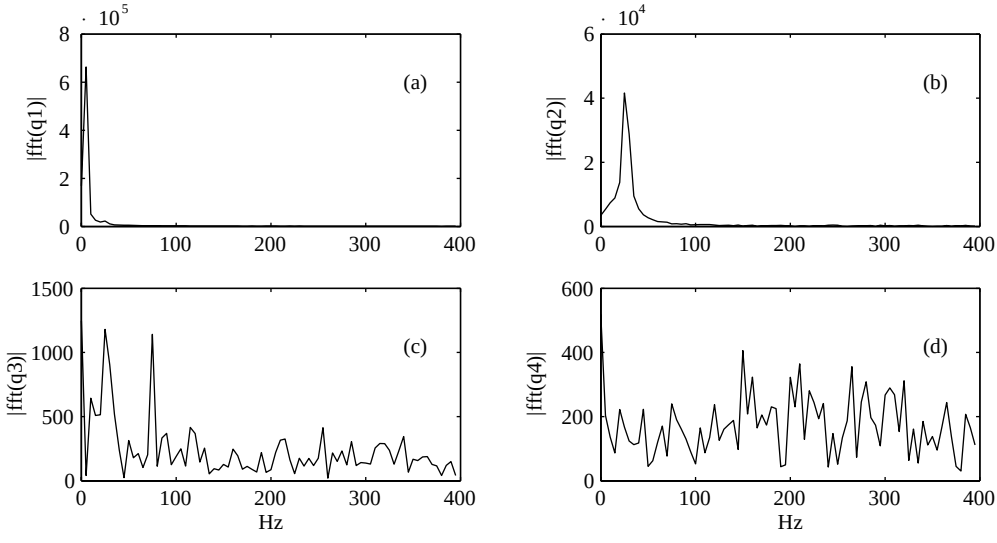

Figure 8. The Fourier transforms of the noise-contaminated proper modal co-ordinate histories $q_i(t)$ for the first four proper orthogonal modes ordered in (a)–(d).

co-ordinate resembles a noisy version of the noise-free case. The fourth, and the higher modal co-ordinates not shown, are mainly noise.

The FFTs of these modal signals are shown in Figure 8. The first three show frequency content consistent with the noise-free case. The fourth, and subsequent modal co-ordinates (not shown), are noisy of similar magnitudes.

Consequently, both the POMs and POVs led to the conclusion that three modes were detectable in the noise-contaminated case.

4. CONCLUSION

POD is often used to assess the number of active modes in a structure by counting the number of POVs above a prescribed threshold. Another perspective considered here is to look at the number of POVs above the noise floor. For nearly linear systems, this gives a good estimate of the number of observable active modes. For non-linear systems, the number of POVs above the noise floor provides an upper bound on the number of active modes.

The noise-floor criterion was applied to the free response of a linear beam. Although some of the modes had very small signal power percentage, the modes represented features of deterministic dynamics. Due to the limited number of independent sensed displacements, the number of detectable modes was evident from the quantum separation of POVs from the noise floor. However, it provided a useful illustration of the basic ideas employed in the noise-floor criterion. We added noise to the data and found that the noise-floor criterion was useful in determining active modes. Modes that were active below the noise level were not recovered.

Proper orthogonal modal co-ordinates can be used to separate the dynamics associated with each POM. In linear systems, if the POMs accurately portray the LNMs (conditions have been provided [13, 14]), the POCs can bring out modal frequencies, and presumably

damping factors. Deviation of the POMs from the LNMs pollutes the modal purity of the POC time histories.

ACKNOWLEDGMENTS

The author is grateful of the support of the National Science Foundation (CMS-9624347), and for the use of data and code generated by M. S. Riaz for the modal analysis study [29].

REFERENCES

1. J. L. LUMLEY 1967 in *Atmospheric Turbulence and Radio Wave Propagation* (A. M. Yaglom and V. I. Tatarski, editors), 166–178. Moscow: Nauka. The structure of inhomogeneous turbulent flow.
2. J. P. CUSUMANO and B.-Y. BAI 1993 *Chaos, Solitons, and Fractals* **3**, 515–535. Period-infinity periodic motions, chaos, and spatial coherence in a 10 degree of freedom impact oscillator.
3. J. P. CUSUMANO, M. T. SHARKADY and B. W. KIMBLE 1993 *Aerospace Structures: Nonlinear Dynamics and System Response, American Society of Mechanical Engineers* **AD-33**, 13–22. Spatial coherence measurements of a chaotic flexible-beam impact oscillator.
4. G. BERKOOZ, P. HOLMES and J. L. LUMLEY 1993 *Annual Review of Fluid Mechanics* **25**, 539–575. The proper orthogonal decomposition in the analysis of turbulent flows.
5. P. FITZSIMONS and C. RUI 1993 *Advances in Robust and Nonlinear Control Systems, American Society of Mechanical Engineers* **DSC-53**, 9–15. Determining low dimensional models of distributed systems.
6. K. MURPHY 1996 *Sixth Conference on Nonlinear Vibrations, Stability, and Dynamics of Structures, Blacksburg, VA.* Using the Karhunen–Loève decomposition to examine chaotic snap-through oscillations of a buckled plate.
7. R. KAPPAGANTU and B. F. FEENY 1999 *Journal of Sound and Vibration* **224**, 863–877. An "optimal" modal reduction of a system with frictional excitation.
8. M. F. A. AZEEZ and A. F. VAKAKIS 2001 *Journal of Sound and Vibration* **240**, 859–889. Proper orthogonal decomposition (POD) of a class of vibroimpact oscillations.
9. X. MA, M. F. A. AZEEZ and A. F. VAKAKIS 2000 *Mechanical Systems and Signal Processing* **14**, 37–48. Nonlinear normal modes and nonparametric system identification of nonlinear oscillators.
10. R. V. KAPPAGANTU and B. F. FEENY 2000 *Nonlinear Dynamics* **23**, 1–11. Part 2: proper orthogonal modal modeling of a frictionally excited beam.
11. K. YASUDA and K. KAMIYA 1997 *Proceedings of the ASME Design Engineering Technical Conferences, Sacramento*, CD-ROM. Experimental identification technique of non-linear beams in time domain.
12. V. LANAERTS, G. KERSCHEN and J. C. GOLINVAL 2000 *Proceedings of the IMAC* XVIII*, San Antonio.* Parameter identification of nonlinear mechanical systems using proper orthogonal decomposition.
13. B. F. FEENY and R. KAPPAGANTU 1998 *Journal of Sound and Vibration* **211**, 607–616. On the physical interpretation of proper orthogonal modes in vibrations.
14. B. F. FEENY 1997 *ASME Design Engineering Technical Conferences, Sacramento*, on CD-ROM. Interpreting proper orthogonal modes in vibrations.
15. G. KERSCHEN and J. C. GOLINVAL 2001 *Journal of Sound and Vibration* **249**(5), 849–866. Physical interpretation of the proper orthogonal modes using singular value decomposition.
16. K. FUKUNAGA 1972 *Introduction to Statistical Pattern Recognition*. New York: Academic Press.
17. E. KREUZER and O. KUST 1996 *Nonlinear Dynamics and Controls*, *American Society of Mechanical Engineers* **DE-91**, 105–110. Proper orthogonal decomposition—an efficient means of controlling self-excited vibrations of long torsional strings.
18. I. T. GEORGIOU and I. B. SCHWARTZ 1996 *Nonlinear Dynamics and Controls, American Society of Mechanical Engineers* **DE-91,** 7–12. A proper orthogonal decomposition approach to coupled mechanical systems.

19. S. HAN and B. F. FEENY 2001 *Journal of Vibration and Control* **8**(1), 19–40. Enhanced proper orthogonal decomposition for the modal analysis of homogeneous structures. Accepted.
20. L. MEIROVITCH 1967 *Analytical Methods in Vibrations*. New York: MacMillian Publishing Co., Inc.
21. D. S. BROOMHEAD and G. P. KING 1986 *Physica D* **20**, 217–236. Extracting qualitative dynamics from experimental data.
22. F. TAKENS 1981 *Lecture Notes in Mathematics.* **898**, 366–381. Detecting strange attractors in turbulence.
23. N. H. PACHARD, J. P. CRUTCHFIELD, J. D. FARMER, and R. S. SHAW 1980 *Physical Review Letters* **45**, 712–716. Geometry from a time series.
24. H. D. I. ABARBANEL, R. BROWN, J. SIDOROWICH and L. TSIMRING 1993 *Reviews of Modern Physics* **65**, 1331–1392. The analysis of observed chaotic data in physical systems.
25. A. I. MEES, P. E. RAPP and L. S. JENNINGS 1987 *Physical Review A* **36**, 340–346. Singular-value decomposition and embedding dimension.
26. A. M. FRASER 1989 *Physica D* **34**, 391–404. Reconstructing attractors from scalar time series: a comparison of singular system and redundancy criteria.
27. M. PALUS and I. DVORAK 1992, *Physica D* **55**, 221–234. Singular-value decomposition in attractor reconstruction: pitfalls and precautions.
28. B. RAVINDRA 1999, *Journal of Sound and Vibration* **219**, 189–192. Comments on 'On the physical interpretation of proper orthogonal modes in vibrations'.
29. M. S. RIAZ and B. F. FEENY 1999 *Proceedings of the ASME DETC, Las Vegas*, CD-ROM. Proper orthogonal decomposition of an experimental cantilever beam.